ISSN 1027-5495. Functional Materials, 25, No.3 (2018), p. 505-515.
doi:https://doi.org/10.15407/fm25.03.505 © 2018 — STC "Institute for Single Crystals"

Application of carbon as a barrier layer in Sc/Si multilayer X-ray mirrors

Yu.P.Pershyn, I.Yu.Devizenko, V.S.Chumak, A.Yu.Devizenko, V.V.Kondratenko

National Technical University "Kharkiv Polytechnic Institute", 2 Kyrpychov Str., 61002 Kharkiv, Ukraine

Received May 30, 2018

X-ray reflectometry in the hard X-ray region (λ = 0.154 nm) was used to investigate the barrier properties of carbon layers 0.2–1.3 nm thick in Sc/Si multilayer X-ray mirrors (MXMs) deposited by DC magnetron sputtering. Precise measurement of the MXM period makes it possible to record volumetric changes in the Sc/C/Si MXM with an accuracy better than 0.01 nm, thus the interaction of the carbon layers with the material of the matrix layers was revealed. The formation of carbide (Si-on-Sc interface) and carbide-silicide (Sc-on-Si nterface) layers was found. The reflectivity of the Sc/C/Si mirrors at the wavelength of ~ 46.9 nm was estimated.
Keywords: multilayer X-ray mirror, carbon barrier layer, layer interaction, EUV region, reflectivity.

Методами рентгеновской рефлектометрии у жесткой рентгеновской области (λ = 0.154 нм) исследованы барьерные свойства углеродных слоев толщиной 0,2–1,3 нм в многослойных рентгеновских зеркалах (МРЗ) Sc/Si, полученных прямоточным магнетронным распылением. Прецизионное измерение периода позволило фиксировать объемные изменения у МРЗ Sc/C/Si с точностью лучше, чем 0,01 нм, за счет чего установлено взаимодействие углеродных слоев с материалом матричных слоев. Обнаружено формирование карбидных (граница Si-на-Sc) и карбидно-силицидных (граница Sc-на-Si) слоев. Сделана оценка отражательной способности зеркал Sc/C/Si на длине волны λ ~ 46.9 нм.

Використання вуглецю як бар'єрного шару у багатошарових рентгенівських дзеркалах Sc/Si. *Ю.П.Першин, І.Ю.Девизенко, В.С.Чумак, О.Ю.Девизенко, В.В.Кондратенко.*

Методами рентгенівської рефлектометрії в жорсткій рентгенівській області (λ = 0.154 нм) досліджено бар'єрні властивості вуглецевих шарів товщиною 0,2–1,3 нм у багатошарових рентгенівських дзеркалах (БРД) Sc/Si, отриманих прямоточним магнетронним розпиленням. Прецизійне вимірювання періоду дозволило зафіксувати об'ємні зміни в БРД Sc/C/Si з точністю краще, ніж 0,01 нм, за рахунок чого встановлено взаємодію вуглецевих шарів із матеріалом матричних шарів. Виявлено формування карбідних (межі Si-на-Sc) і карбідно-силіцидних (межі Sc-на-Si) шарів. Проведено оцінку відбивної здатності дзеркал Sc/C/Si на довжині хвиль λ ~ 46,9 нм.

1. Introduction

Scandium-silicon multilayer X-ray mirrors (MXMs) have high theoretical reflectance ($0.3 < R < 0.6$) at normal incidence in the extreme ultraviolet (EUV) wavelength range (λ = 35–50 nm) [1], but the presence of mixed interlayers on interfaces reduces these values at least by 30 %. The suppression of interlayer interaction would increase their reflectance and enhance device efficiency on their base.

Barrier layers effectively prevent interlayer interaction and increase the efficiency and stability of mirrors as it was shown earlier [2, 3]. Various materials of the barrier layers were used to improve the thermal stability of the Sc/Si MXMs:Cr [4], B_4C [5], ScN [5]. The insertion of these layers increased the stability of the MXM, but at the same time led to a slight decrease in their reflectivity in the EUV region. However, in such studies the measurement of the mirrors reflectivity was the main tool for evaluating barrier properties, but the structure of the barrier layers, their "transparency", the critical thickness of the barrier completely isolating the matrix layers, were either not considered at all or evaluated indirectly.

In this paper we investigated the effect of carbon barrier layers on the mixing of Sc and Si matrix layers with a successive change in the thickness of the barrier layers (t_C), as well as their effect on the reflectivity of the Sc/Si MXM in the soft X-ray region near $\lambda \sim 47$ nm. A capillary discharge laser operates at this wavelength [6], which is currently one of the brightest sources of EUV [7]. We are going to optimize the X-ray optical properties of the Sc/Si MXMs with carbon, which is a new material for this material pair. It has the highest melting point (3823 K) as compared with barrier materials mentioned above, that facilitates decreasing in the diffusion processes activity at the interlayers. Previously, carbon barriers have been used to prevent interlayer interaction in the Mo/Si MXMs [8–11], where the interaction scales are at least 3 times smaller than in the Sc/Si system. Therefore, we expect here a decrease in the thickness of the mixed layers. Besides, as it is shown earlier [8], carbon barriers significantly increase the MXM stability, so this work is the first step in the creation of the stable Sc and Si based MXMs.

2. Experimental

Samples of the Sc/Si multilayers were prapared by direct-current magnetron sputtering. The targets were scandium, silicon and carbon plates with a diameter of ~100 mm and a purity of 99.3 %, 99.99 % and 99.9 % respectively. The silicon target was a (111)Si single crystal wafer. During each experiment, the currents on all magnetrons and the argon pressure (2.4 mTorr) were kept constant to ensure a constant rate of deposition. The deposition rates for scandium, silicon and carbon were ~ 0.38 nm/s, ~ 0.52 nm/s and ~ 0.13 nm/s, respectively. Mirrors were deposited onto silicon or float glass substrates with surface roughness of 0.3–0.5 nm.

The samples were measured at X-ray diffractometer DRON-3M equipped with a primary crystal-monochromator (110)Si to extract $CuK\alpha_1$ radiation ($\lambda = 0.154$ nm) only from the X-ray spectrum created by a copper tube. The use of such a scheme ensures the formation of an X-ray beam with a divergence of ~ 0.15° and the intensity of ~10^6 cps, which allows recording reflected radiation in a dynamic range of intensities covering 6 orders of magnitude. The phase composition of the samples was estimated at another diffractometer with a graphite analyzer that provided the emission of $CuK\alpha$ radiation without separation of the $K\alpha$-doublet ($\lambda = 0.1542$ nm) with a divergence of ~ 0.5° and the intensity of ~ 10^7 cps.

The periods of the produced MXMs were calculated by the Bragg formula taking into account the refractive index and with involvement of the least squares method for all small-angle diffraction maxima.

Reflectivity of mirrors was estimated using the IMD program [12], which uses the Fresnel formulas and the optical constants of individual layers. Optical constants for Sc were taken in [13, 14], and those for layers of complex composition were calculated on the basis of known optical constants of pure components.

3. Results and discussion

We fabricated a series of samples in which the carbon layers thickness successively varied from 0.2 nm to 1.3 nm for both interlayers in turn.

In order to trace the influence of the carbon barrier layers on the interlayer interaction only, we deposited a test multilayer and a reference multilayer simultaneously on the same substrate. The test multilayer was always deposited on top. The reference multilayer was a Sc/Si multilayer without barriers, and the test multilayer was the same Sc/Si multilayer but with barrier layers. This was done to exclude the effect of a small drift in the Sc and Si deposition rates for different experiments. Deposition times of the main components exceeded 10 seconds. If we assume that in different experiments there will be change in deposition rates of 0.01 nm/s only it can lead to a period change of more than

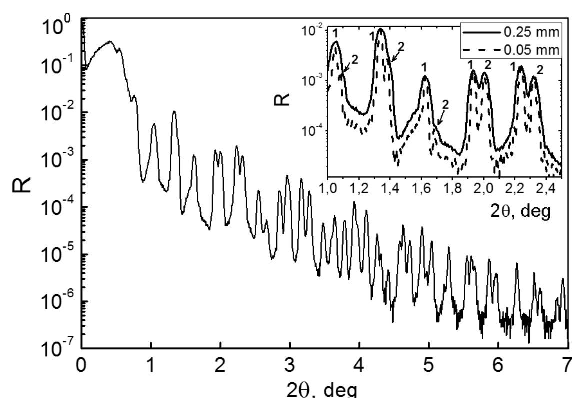

Fig. 1. X-ray diffraction pattern from a multilayer sample consisting of two multilayer stacks: Sc/Si/20 (d = 26.861 nm, the number of periods is 20); and Sc/Si/C/15 (d = 27.156 nm, the number of periods is 15) with the carbon layers ~ 0.36 nm thick. The inset shows an enlarged part of the diffractogram in the range of angles $2\theta = 1-2.5°$ demonstrating the separation of peaks with the narrow slit.

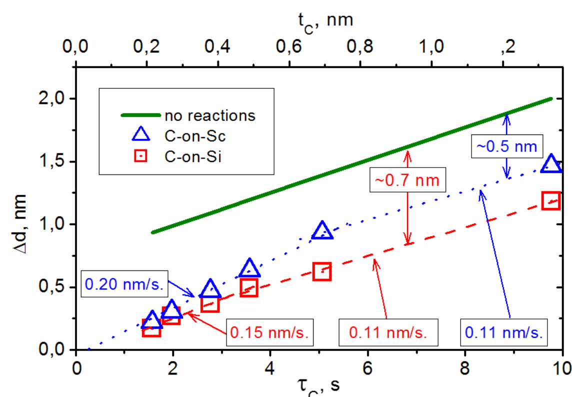

Fig. 2. Experimental dependence of the period increment, Δd, (triangles and squares) of the Sc/Si MXM on the deposition time of the carbon layer. The solid line indicates the expected values of Δd in the absence of any interaction in the multilayer system.

±0.2 nm, which is comparable to either a thickness or an increment for carbon layers. Differences (Δd) in the periods between the test and reference multilayers should reveal the degree of interaction between the original components, and the accuracy of its measuring-in is defined by the accuracy of measuring the period values and the accuracy of reproduction of barrier deposition rates.

3.1. Sc/Si multilayers with barrier layers

An X-ray diffraction pattern (λ = 0.154 nm) from a multilayer sample containing both the test and reference multilayer stacks is shown in Fig. 1. The periods of deposited stacks were ~ 27 nm, and the difference is ~ 0.2 nm, so at small angles the diffraction maxima from different stacks cannot be separated with a standard slit. As can be seen from Fig. 1 this happens for the first five maxima ($2\theta < 2°$), then the maxima for different stacks can be divided. The accuracy of the MXM period determination depends on the number of maxima, so we slightly improved the measurement conditions of multilayer samples to separate the maxima at angles $2\theta < 2°$. To do this, we reduced the slit to 0.05 mm instead of the standard 0.25 mm slit right before the detector. The results of this measurement are shown in an inset to Fig. 1. It can be seen that the narrower slit made it possible to divide maxima and determine the angular positions of three additional diffraction maxima (dashed line) as compared to the standard slit (solid line). As a result, the accuracy of the period determination increased by a factor of ~ 3 (at least for the lower stack) and was ±0.005 nm.

We found the difference in the periods (Δd) between the test multilayer (d) and the reference one (d_0) and plotted its dependence on the deposition time (τ_C) of the carbon layer in Fig. 2 for the interfaces of Sc-on-Si (squares) and Si-on-Sc (triangles). As can be seen from the figure, the deposition of carbon layers leads to the period increase for the studied samples, and this increase is larger when the barrier layers are deposited on the scandium layers compared to the silicon layers. The straight lines drawn through the experimental points reveal jogs on both relationships. Slope ratios for them give the rate of this change. Thus for carbon deposited on scandium, the growth of the period in the first region ($\tau_C < 5$ s) occurs with a deposition rate of 0.203±0.001 nm/s, and for carbon deposited onto silicon ($\tau_C <$ 3.1 s) the deposition rate is 0.15±0.01 nm/s. A more active period growth with increasing carbon thickness at the Si-on-Sc interfaces probably indicates a better ability of carbon layer to block the Si and Sc layers at these interlayers. In the second regions the similar rates of the period growth are observed for both dependences: ~ 0.11 nm/s.

The expected values of Δd for the case when the interaction between the main components and the material of the barrier

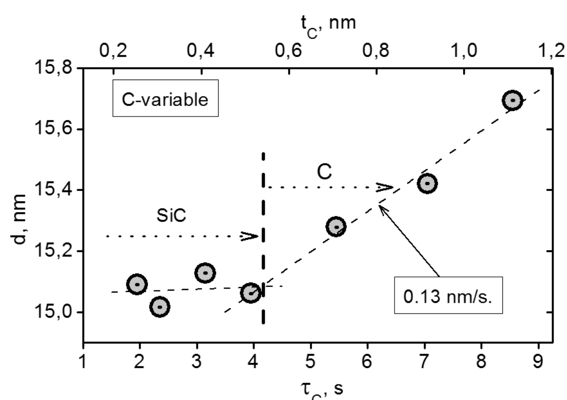

Fig. 3. The period of the Si/C multilayer system versus the deposition time of the carbon layer at a fixed thickness of silicon layers (t_{Si} ~ 15 nm).

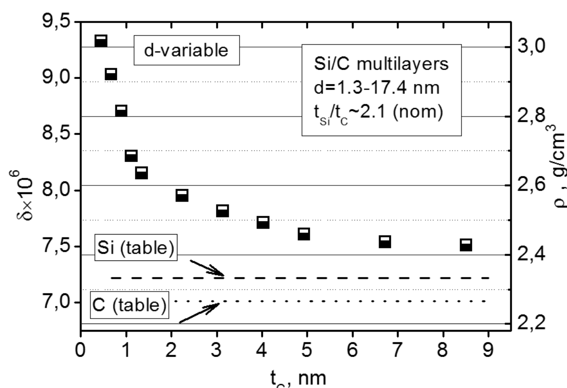

Fig. 4. Increment δ of the refractive index ($n = 1 - \delta$ (left axis) and density ρ (right axis) for Si/C multilayer systems in the X-ray region ($\lambda = 0.154$ nm) against carbon layer thickness. The periods of Si/C multilayer systems varied from 1.3 to 17.4 nm.

layer is absent were drawn in the form of a solid line in Fig. 1. These values were calculated on the basis of the absence of mixed ScSi interlayers 3 nm thick and the deposition rate of carbon layers. Although it is known that in the Sc/Si multilayer mixed interlayers can reach a thickness of ~ 5 nm [15], we started plotting with a minimum thickness. Since the nominal thicknesses of Sc and Si are the same for all samples, and only the thickness of the carbon layer changes, the slope ratio should correspond to the deposition rate of carbon (0.13 nm/s). In this connection we rescaled the top axis of abscissa in thickness of carbon layer. Fig. 2 shows that the difference in Δd in the absence of any interaction (solid line) and the experimental Δd for the second region ($\tau_C > 3.1$ s) is at least 0.5 nm. Significant difference between the expected values and the experimental indicates that either the carbon layer does not prevent the interaction of Sc and Si completely for the thicknesses under study, or it reacts with the main components.

3.2. Si/C multilayers

In order to figure out the possible interaction between the layers of carbon and silicon, we conducted a similar study for a multilayer system in which the components were only Si and C. In the first experimental series the silicon thickness remained fixed (t_{Si} ~ 15 nm), and the carbon thickness changed only. Results of the measurements for the period, d, of the Si/C multilayers versus the carbon layer deposition time are shown in Fig. 3. At the initial stage ($\tau_C < 4.1$ s) the period is stable near 15.1 nm, and then it begins growing at $\tau_C >$ 4.1 s. A straight line drawn through the last 4 points allows determining its growth rate which is ~ 0.13 nm/s in exact correspondence with the previously measured carbon deposition rate. This coincidence indicates that pure carbon layers appear in the Si/C multilayers after ~ 4 seconds of deposition. This makes it possible to change the temporal scale to a thickness one, which is shown on the top axis of abscissa. Taking into account the scatter of the periods at the initial stage ($\tau_C < 4.1$ s) we can estimate that the pure carbon appears in Sc/C multilayers when carbon layer thickness reach 0.53±0.05 nm. This value is somewhat larger than our preliminary estimated one (~ 0.36 nm), obtained above in Fig. 2. However, if we take into account that it can be two carbide interlayers in Si/C multilayers, this discrepancy can only indicate that another SiC interlayer is being formed. Judging from the obtained thicknesses of carbon, it may be of a different thickness.

Thin carbon layers can react with silicon layers and according to the literature [16] form silicon carbide. The formation of carbide is indicated by the critical angle increase with the period decrease for another series of Si/C multilayer samples (Fig. 4). Here the multilayer period varied from 1.3 to 17.4 nm while the nominal thickness ratio of the layers was kept constant. When plotting the graph in Fig. 4 we followed the practice to build every possible parameter in a functional dependence on the thickness (or the deposition time) of the carbon layers, although in this series the thickness of the silicon layers certainly changed. The total

increase in coating density, which was estimated from the critical angle, exceeded 20 % with respect to pure components. It is possible to estimate the density of a material or a coating from the critical angle using the following formulas [17]:

$$\delta = \theta^2_{cr}/2, \quad (1)$$

$$\delta = 2.701 \cdot 10^{-6} \frac{\rho}{A} f_1 \lambda^2, \quad (2)$$

or

$$\delta = 6.405 \cdot 10^{-8} \frac{\rho}{A} f_1 (\text{for } \lambda = 0.154\ nm), \quad (3)$$

where δ is the real part of the refractive index increment $(1 - n)$ of the substance in the X-ray region $(n = 1 - \delta)$; θ_{cr} is the critical angle in the total external region for X-rays (in radians); ρ is the matter density (g/cm^3); A is atomic weight; f_1 is the atomic factor of X-ray scattering by atoms of a given type; λ — the wavelength of X-ray radiation (nm).

The atomic scattering factors of light atoms (the first 3 periods of the Periodic Table of the Elements) in the hard X-ray region ($\lambda = 0.154$ nm) roughly correspond to the number of electrons in the atom or, simply, to the atomic number Z: for example, $f_1^{C} = 6.01917$ ($Z = 6$), $f_1^{Si} = 14.2969$ ($Z = 14$). The ratios f_1/A [in formulas (2) and (3)] for silicon and carbon are close to 0.5 and differ from each other just by 0.4 %: 0.5011 (C) and 0.5090 (Si). Based on this fact, we rewrote equation (3) as:

$$\delta = 3.235 \cdot 10^{-6} \rho, \quad (4)$$

or

$$\rho = 1.546 \cdot 10^{5} \cdot \theta^2_{cr}. \quad (5)$$

We calculated the densities of the Si/C multilayer systems for δ shown in Fig. 4 using formula (5). We found that δ for Si/C samples increase at least by 24 %. As follows from the formula (4), the density, ρ, is related to δ linearly, so we added one more ordinate axis (on the right) to the same graph, graduated on the density scale. Figure 4 shows that the densities of multilayer coatings exceed the Table densities of pure components for both Si (2.332 g/cm^3) and C (2.266 g/cm^3) (shown by horizontal lines) over the entire range of the studied periods. For small periods ($d < 2.5$ nm, the first three values), the density of multilayer samples approaches the tabular density of SiC (3.22 g/cm^3). The interaction of carbon and silicon layers is also evident from the fact that the peaks for Si/C multilayer with the smallest period ($d \sim 1.3$ nm) disappear, since there should be practically no pure carbon or pure silicon in the samples. For the observed level of interlayer roughness ($\sigma < 0.45$ nm), the estimated reflectivity of the Si/C samples should be at least $5 \cdot 10^{-6}$, and it can be easily observed at the X-ray diffractometer, not speaking of the case that SiC/Si or SiC/C multilayers should have a reflectivity of $R > 2 \cdot 10^{-5}$ even with a distortion in the SiC fraction in the period up to $\beta \sim 0.9$.

Both series of produced samples have an amorphous structure throughout the studied range of thicknesses, in other words, both the layers of carbon and silicon themselves and also the product of their reaction at interlayers, i.e. silicon carbide are amorphous. The maximum density of multilayer samples is less than the tabulated SiC density by only ~ 6 %. We suggest that amorphousness also contributes to a decrease in the density of reaction products.

Thus, it can be concluded that carbon interacts with the silicon layer even during the deposition process; its interaction thickness is ~ 0.53 nm; the composition of the interacted zones is silicon carbide with a density close to the table one; the total carbide thickness should be 1.24±0.12 nm.

3.3. Sc/C multilayers

We made a Sc/C sample with two multilayer stacks differing in the carbon layer only to study the interaction of scandium and carbon layers. The nominal scandium thickness in both stacks was constant ~ 2.8 nm. The nominal carbon thicknesses were ~ 4.4 nm and ~ 5.9 nm. An X-ray diffraction pattern from this sample is shown as small circles in Fig. 5. The solid and dotted lines show the calculated curves, which were fitted to the experiment one using the thickness, composition, density and roughness of the layers as fitting parameters. These curves represent the extreme variants describing the structure of the produced sample, namely: Sc/C and ScC/C. In the first case, the thickness of the scandium layers was ~ 2.8 nm, which corresponds to the nominal value. In the second case, we assumed that the scandium layers react with carbon, forming scandium carbide ScC with a thickness of ~ 2.9 nm. We also tried to fit the experimental curves with other

carbides ($Sc_{15}C_{19}$) in accordance with the Sc–C state diagram, including the case in which the scandium layers react with carbon ones partially, i.e. with the involvement of a four-layer model for the multilayer construction, for example ScC/Sc/ScC/C, but all of them, depending on the proportion of pure scandium in the period, enter into these variants as intermediate.

As can be seen from Fig. 5, both models give close curves in the range of angles 2θ > 1.5° while fitting. However, according to the first model (the Sc/C system), it is not possible to fit the first maxima from both stacks in the range of angles 2θ ~ 1.3°: these maxima are always lower than the experimental ones for any fitting parameters. This is clearly seen in an inset to Fig. 5. When fitting according to the second model (ScC/C), these maxima fit easily. The main reason for this behavior in the fitting curves is a noticeable difference in the densities of Sc (~ 3 g/cm^3) and ScC (~ 3.6 g/cm^3). A higher density of ScC causes a higher reflection coefficient in the hard X-ray region (λ = 0.154 nm).

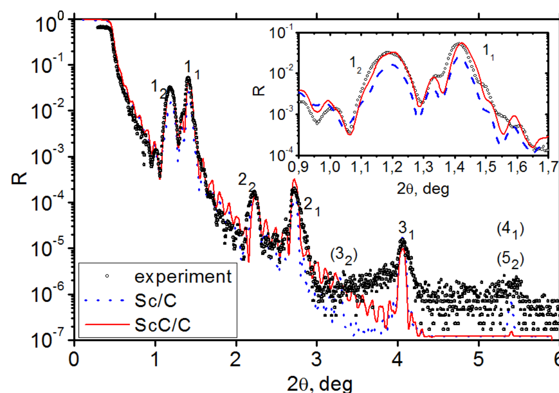

Fig. 5. X-ray diffraction pattern (λ = 0.154 nm) for Sc/C multilayer sample consisting of two stacks (d_1 = 6.53±0.01 nm, d_2 = 7.99±0.01 nm) differing in the thickness of the carbon layer only. Numbers indicate the order of reflection; subscript indices refer to the number of a multilayer stack. The insert shows an enlarged image of the same diffrac-

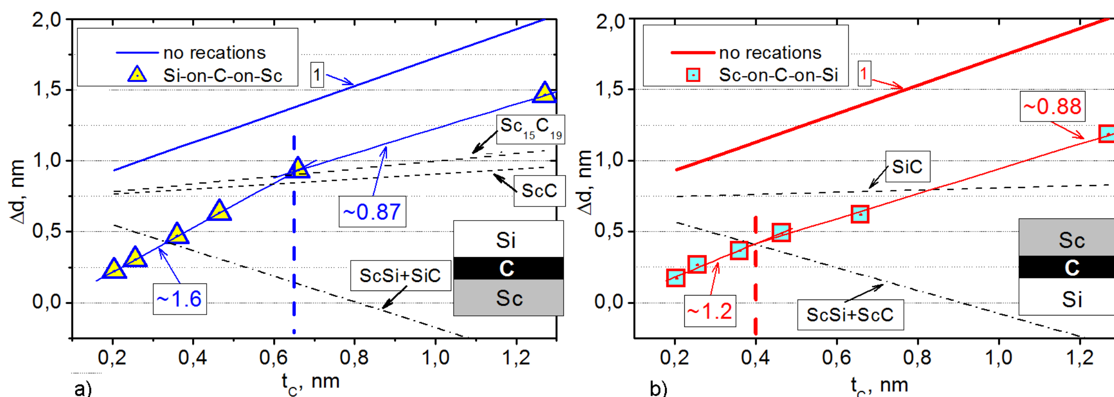

Fig. 6. The experimental dependence of the period contraction, Δd, on the thickness of the carbon layer, t_C, for the interlayers (a) Si-on-Sc (triangles) and (b) Sc-on-Si (squares). Thick solid lines show the calculated data for the case of absence of any interaction between the components.

The fact that the sample under study has an amorphous structure also indicates the interaction of the layers. According to our data, scandium thicker than ~ 1.8 nm should already be crystalline. The absence of diffraction lines for crystalline scandium layers ~ 2.8 nm thick indicates that scandium should interact with carbon at least partially.

Thus, the tendency of carbon interaction with scandium layers is revealed, and the carbide layer thickness can reach ~ 2.9 nm.

3.4. Estimation of the composition and thickness of the mixed zones

Now, knowing that carbides can be formed in the Sc/C/Si multilayer system, we estimate the thickness and composition of the mixed zones. To start with, we rebuild the experimental data in Fig. 2 in the coordinates Δd = $f(t_C)$. In Fig. 6 triangles are the experimental data for the Si-on-Sc interfaces (Fig. 6a) and squares are for the Sc-on-Si interfaces (Fig. 6b). The experimental dependences in Fig. 6 have two regions with different slope ratio for the experimental points: ~ 1.6 and ~ 0.87 (Fig. 6a); ~ 1.2 and ~ 0.88 (Fig. 6b). The boundaries of these regions are marked with vertical dashed lines.

Table 1. Molar volumes of various substances, calculated on the basis of tabulated data

No.	Materials	Density, (ρ), g/cm^3	Molar mass, g	Molar volume, (V), cm^3
1	Sc	3.02	44.9559	14.88606
2	Si	2.332	28.0855	12.04352
3	C	2.266	12.011	5.30053
4	SiC	3.22	40.0965	12.45233
5	ScC	3.6	56.9669	15.82414
6	$Sc_{15}C_{19}$	3.606	902.548	250.29
7	Sc_5Si_3	3.299	309.036	93.67566
8	ScSi	3.363	73.0414	21.71912
9	Sc_3Si_5	3.393	275.2952	81.13622

Table 2. The molar volumes of various reactions possible in the Sc–Si interlayers with the introduction of carbon layers

No.	Chemical reactions	Molar volumes of components, cm^3	$\Delta V/V$	$1 - \Delta V/V_C$
1	Si + C = SiC	12.044 + 5.301 → 12.452 (4.893)	−0.282	0.077
2	Sc + C = ScC	14.886 + 5.301 → 15.824 (4.363)	−0.216	0.177
3	15Sc + 19C = $Sc_{15}C_{19}$	223.291 + 100.71 → 250.291 (73.711)	−0.228	0.268
4	2Si + Sc + C = ScSi + SiC	24.09 + 14.89 + 5.3 → 21.72 + 12.45 (10.1)	−0.228	−0.905
5	6Si + 3Sc + C = Sc_3Si_5 + SiC	72.26 + 44.66 + 5.3 → 81.14 + 12.45 (28.64)	−0.234	−4.403
6	4Si + 5Sc + C = Sc_5Si_3 + SiC	48.18 + 74.43 + 5.3 → 93.68 + 12.45 (21.78)	−0.170	−3.109
7a	2Sc + Si + C = ScSi + ScC	29.77 + 12.04 + 5.3 → 21.72 + 15.82 (9.57)	−0.203	−0.806
7b	16Sc + Si + 19C = ScSi + $Sc_{15}C_{19}$	238.2 + 12.04 + 100.7 → 21.72 + 250.3 (78.93)	−0.225	0.216
8a	4Sc + 5Si + C = Sc_3Si_5 + ScC	59.54 + 60.22 + 5.3 → 81.14 + 15.82 (28.11)	−0.225	−4.302
8b	18Sc + 5Si + 19C = Sc_3Si_5 + $Sc_{15}C_{19}$	268 + 60.22 + 100.7 → *Б44 Φ* 4[*B*81.14 + 250.3 (97.46)	−0.227	0.03
9a	6Sc + 3Si + C = Sc_5Si_3 + ScC	89.32 + 36.13 + 5.3 → 93.68 + 15.82 (21.25)	−0.163	−3.009
9b	20Sc + 3Si + 19C = Sc_5Si_3 + $Sc_{15}C_{19}$	297.7 + 36.13 + 100.7 → *Б44 Φ* 4[*B*93.68 + 250.3 (90.6)	−0.208	0.100

Then, on the basis of tabular densities and atomic masses, we made preliminary calculations for molar volumes of substances that can be formed in multilayer samples (Table 1). Here we considered two scandium carbides: ScC and $Sc_{15}C_{19}$ (No. 5 and No. 6), as they are presented in the phase equilibrium diagram. The latter of these carbides is sometimes represented in the literature [18] as Sc_3C_4. We performed calculations for both modifications of this carbide, but since the obtained values are close for these modifications, we omitted the results of calculations for Sc_3C_4.

Next, we considered the various types of reactions that can occur at interlayers from the viewpoint of volumetric changes taking into account the data of Table 1. The results of calculations together with the useful ratios are given in Table 2. Here the reactions are shown in the 2nd column; the molar volumes of the substances involved in the reaction (volumetric contraction in absolute units is indicated in parentheses) is in the 3rd column; the 4th column shows volumet-

ric changes, ΔV, due to the reaction in relative units in relation to the volume, V, of the initial components; the 5-th column displays the ratio $(V_C - \Delta V)/V_C = 1 - \Delta V/V_C$, which corresponds to the slope ratio in Fig. 6. In all the cases listed in the Table 2, we assumed that the interaction of the matrix Sc and Si layers is absent. We did not consider the triple compounds of Sc–Si–C, since we are not aware of the existence of such compounds. It should be noted that in Table 2 the reactions leading to the formation of silicides and carbides are divided into 2 groups according to different interlayers. Reactions No. 4–6 correspond to the Si-on-Sc interfaces for which silicon is deposited on a scandium carbide or scandium layer coated with carbon, and reactions No. 7–9 to the Sc-on-Si interfaces where scandium atoms are deposited on silicon, coated with carbon, or on SiC. Such dividing will facilitate further analysis.

Table 2 shows that the volumes of components in the right and left parts of each reaction (column 3) are not equal, i.e. all of them react with a volume decrease which agree with the experimental data (see Fig. 6). The magnitudes of this decrease are indicated in parentheses. For example, for reaction No. 1, the interaction of 1 mole of silicon (~ 12 cm^3) and 1 mole of carbon (~ 5.3 cm^3) results in the production of 1 mole of silicon carbide SiC (~ 12.5 cm^3) and volume contraction of ΔV ~ 4.9 cm^3, which is ~ 0.28 of the volume of the initial products of the reaction. The reaction of carbide formation of scandium is accompanied by less shrinkage: 0.21–0.23 (reactions 2 and 3, Table 2). We suppose that this difference can be one of the reasons for the smaller volume contraction found forthe Sc/C/Si MXM with carbon deposition on the Si-on-Sc interfaces (~ 0.5 nm) compared with the Sc-on-Si ones (~ 0.7 nm), which are observed in Fig. 2.

Now, comparing the experimental data shown in Fig. 6 with the calculations in Table 2, we will try to restore the growth pattern of the interlayers with carbon barriers. The slope ratio for the experimental dependences approximated by the straight lines in Fig. 6 must correspond to $(1 - \Delta V/V_C)$ of Table 2 (last column). Comparing these data, we can make an estimation of the barrier layer composition and its barrier properties. Initially we consider the first regions in Fig. 6, namely ones with $t_C <$ 0.65 nm (Fig. 6a) and $t_C <$ 0.4 nm (Fig. 6b). If we confine ourselves only to carbides (the first 3 reactions in Table 2), then it can be seen that all the $(1 - \Delta V/V_C)$ values are less than the experimental ones of ~ 1.6 and ~ 1.2. Considering reactions with the formation of silicides (reactions 4–12), one can observe reactions with both positive and negative values. The presence of negative values of $(1 - \Delta V/V_C)$ means that the volumetric contraction for these reactions exceeds the thickness of the added carbon layer, i.e. the total volume of the substance after the reaction decreases even without accounting for carbon. In Fig. 6 this should appear in the form of negative slopes for $\Delta d(t_C)$, i.e. Δd should decrease with t_C increasing. This can be observed for reactions in which ScSi and one of the scandium carbides are formed, they are plotted in Fig. 6a,b as examples. Positive values of $(1 - \Delta V/V_C)$ for the reactions presented in the Table 2 do not exceed the similar values for the reactions of carbide formation. In other words, according to formal characteristics, none of the reactions is suitable in explicit form to explain the experimental dependences $\Delta d(t_C)$.

In Fig. 6a, we also plotted the expected dependences $\Delta d(t_C)$ for the case when carbon carbide layer (ScC or $Sc_{15}C_{19}$) is formed in the scandium layers and blocks the interaction of the Si and Sc matrix layers completely (dashed lines). The graphs have a positive slope and cross the experimental dependence in the region of the jog. The jog on the dependences $\Delta d = f(t_C)$, i.e. the boundaries of adjacent regions (Fig. 6a), must correspond to the moment of complete isolation of the matrix layers. The use of this fact allows us to conclude that the formation of scandium carbide occurs in the first section of the Si-on-Sc interface (Fig. 6a), which blocks the interaction of the Sc and Si matrix layers below t_C ~ 0.65 nm partially. As a result the Δd values grow according to a law different from the expected one for reactions No. 2–3 (Table 2). The linear dependence in this section indicates that: 1) either the permeability of the carbide layer for silicon decreases with thickness increasing; 2) or the carbide layer is discontinuous and became solid with the appearance of an additional amount of carbon. In the second case, this should be seen in an increased interfacial roughness: in the absence of the carbide layer, silicon can penetrate into the scandium to a depth of 3 nm. The roughness should lead to the disappearance of diffraction maxima for a

Table 3. Formation enthalpy of various compounds, reduced to one mole of scandium (silicon)

No.	Chemical reaction	ΔH (25°C), kJ/(mol·K)	No.	Chemical reaction	ΔНБ \ИНВ (25°C), kJ/(mol·K)
1	Si + C = SiC	−66.1	7	Sc + 0.5SiC = 0.5ScSi + 0.5ScC	−125.2
2	Sc + C = ScC	−151.8	8	Sc + 0.36SiC = 0.36ScSi + 0.64$ScC_{0.56}$	−126.4
3	Sc + 0.56C = $ScC_{0.56}$	−142.1	9	Si + ScC = ScSi + C	−12.8
4	Sc + Si = ScSi	−164.6	10	Si + ScC = SiC + Sc	85.7
5	Sc + SiC = ScSi + C	−98.5	11	Si + 0.5ScC = 0.5ScSi + 0.5SiC	−39.5

Sc/C/Si multilayer sample at angles $2\theta > 2°$, which is not observed in Fig. 1. Most likely, the carbide layer is continuous and up to ~ 1.9 nm (~ 0.65 nm of carbon) is "semitransparent" for silicon atoms. In this case, the interfacial roughness can be kept low.

The expected dependence $\Delta d(t_C)$ for the case when carbon is deposited on silicon layers and forms SiC is plotted as a dashed line in Fig. 6b. It has a positive slope ratio and crosses the experimental dependence in the region of carbon thickness of t_C ~ 0.86 nm, which is far beyond the jog (t_C ~ 0.4 nm). The intersection occurs in the second region, where full isolation of the matrix layers is already expected, and there are no specific features in the plot. However, if we consider the dependence $\Delta d(t_C)$ for the case of the silicide-carbide formation (reaction No. 7a), i.e. when scandium reacts with both components of SiC (in Fig. 6b a dotted line with a negative slope ratio), it can be seen that there is also an intersection with the experimental dependences at the boundary of the two regions. Contraction in reaction No. 7a at t_C ~ 0.4 nm is ~ 0.3 nm, which is noticeably less than the possible increase (~ 0.73 nm) in the Sc/Si multilayer period due to exclusion of interaction at one of the interlayers. Therefore, despite the expected contraction in the carbide-silicide reaction, an increase in volume can still be observed in the experimental dependence. A large number of diffraction maxima for samples with a carbon layer at the Sc-on-Si interlayer, as in the case of Si-on-Sc interfaces, indicates that the carbide-silicide interlayers are solid but "semitransparent" up to t_C ~ 0.4 nm.

The appearance of the second region with a different slope ratio ($\Delta d/t_C$ ~ 0.9) indicates that the character of the carbon interaction with matrix layers has changed. In these regions, pure carbon could appear, but the slope ratio is less than one and it indicates that carbide reactions occur partially here.

A slight discrepancy between the calculated data and the experiment may be due to the difference in the densities of the substances formed from the tabulated, non-stoichiometric compounds or a mixed type of reactions. In any case, we suggest that in the initial stage of carbon deposition (t_C < 0.65 nm and t_C < 0.4 nm), the basis for the composition of the mixed zones at both interfaces of the Sc/C/Si multilayer system are substances in reactions No. 2–3 and No. 7a.

These results are also supported by calculations of the thermal effects accompanying the reactions represented in Table 3. Here the enthalpies of formation are reduced to one mole of scandium or one mole of silicon in those reactions where scandium is absent. The formation of carbides, as can be seen from Table 3, is thermodynamically preferable in Sc–C and Si–C systems. In addition, scandium compounds: ScC, $ScC_{0.56}$ (i.e. $Sc_{15}C_{19}$) and ScSi (reactions 2–4) are more stable than SiC carbide (reaction 1). Although scandium is able to replace silicon or carbon in the SiC compound (reactions 5 and 6), nevertheless, as it is shown by reactions 7 and 8, a variant is preferred where scandium breaks down the SiC molecule and reacts with both components. For the same reason, silicon is able to replace carbon in scandium carbide (reaction 9), but is unable to replace scandium (reaction 10). However, as shown by reactions 11 and 12, it is thermodynamically more preferable for silicon to react with scandium carbide, forming ScSi and SiC, compared to carbon replacement (reaction 9).

The calculations given in Table 3 also show that the reaction of the atoms deposited on the already formed carbide with the atoms of the carbide itself is energetically preferable (reactions No. 7–8 and 11–12), and the thermal effect of the interaction of

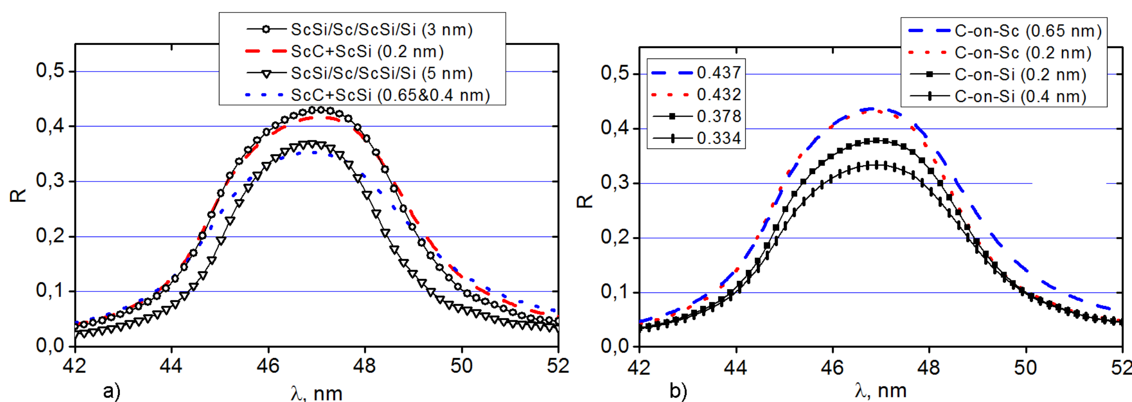

Fig. 7. Estimated reflectance, R, for the Sc/C/Si MXM in the wavelength range $\lambda = 42$–52 nm at normal incidence. (a) Barriers are located on both interlayers: 0.2 nm thickness (dash line); thickness of barrier layers 0.65 and 0.4 nm (see text) (dot line); the reference curves are Sc/Si MXMs with silicide interlayers of 3 nm (circles) and 5 nm (triangles) without barriers. (b) Barriers are located only at one interlayers: barrier thickness of 0.2 and 0.65 nm (Si-on-Sc interfaces); barrier thickness 0.2 and 0.4 nm (Sc-on-Si interfaces).

scandium with silicon carbide (reactions No. 7–8) is at least twice the heat released during the interaction of silicon with scandium carbide (reactions No. 11–12).

From the data given in this subsection, it can be concluded that the formation of interlayer Si–Sc (Sc–Si) boundaries involving carbon occurs in two stages. At the first stage, the deposited carbon reacts with a layer of scandium (silicon) and forms an interlayer of scandium carbides (silicon carbides). If the deposited carbon layer is thin ($t_C < 0.4$–0.65 nm), the subsequent layer of silicon (scandium) can react with both the carbide layer and the underlying scandium (silicon) layer and form silicides. As the thickness of the carbon layer increases, it becomes "opaque" for silicon atoms (scandium), and silicon atoms (scandium) can only react with a layer of carbides. For thick carbon layers ($t_C > 0.4$–0.65 nm), when a layer of pure carbon appears on the surface of the carbide layer, the deposited silicon atoms (scandium) partially react with it forming a layer of silicon carbide (scandium carbide).

3.5. Estimation of reflectivity in EUV region

The minimum thickness of carbon layers in our experiments is ~ 0.2 nm, which, as follows from Table 2 (reactions 2–3), should correspond to the thicknesses of scandium carbides of ~ 0.5–0.6 nm and the thicknesses of carbide-silicide layers of ~ 1.4 nm (reaction 7a). Barrier layers are semitransparent at such thicknesses. By the difference between the expected value of Δd for the barrier of established composition and the actual value of Δd, it is possible to estimate the thickness of the ScSi silicide, which is formed in such cases. For the minimum carbon thicknesses (~ 0.2 nm) they are ~ 2.2 nm (Fig. 6a) and ~ 1.6 nm (Fig. 6b). The boundaries of adjacent regions are at t_C ~ 0.65 nm (Fig. 6a) and t_C ~ 0.4 nm (Fig. 6b), which corresponds to the mixed zones of ~ 1.6–1.9 nm and ~ 2.6 nm. The formation of monosilicidal layers is not expected in this case. We used these data as input parameters to calculate the reflectivity of Sc/C/Si multilayer mirrors in the 42–52 nm wavelength range in order to evaluate the effectiveness of the barrier layers. We used tabular material densities, interlayer roughness $\sigma = 0.5$ nm and a grazing incidence angle $\theta = 85°$ in the calculations. The top layer was silicon with a surface oxide 2.5 nm thick in every sample.

The plot of reflectivity versus wavelength for mirrors with barrier layers on both interface boundaries is shown in Fig. 7a: with nominal carbon thickness ~ 0.2 nm (dash line); various carbon thicknesses (0.65 and 0.4 nm) at different boundaries which should ensure complete isolation of the matrix elements (dot line). As a reference, we calculated the Sc/Si multilayer mirrors with two ScSi interlayers 3 nm thick (circles) and 5 nm thick (triangles). The peak reflectivity is reduced from R ~ 0.43 to R ~ 0.417 with the insertion of thin carbon layers in comparison with the MXM with 3 nm interlayers. The reflectivity decreases further to R ~ 0.353 with increase of barrier thickness. However, the MXM with thin barrier layers keep advantage over the Sc/Si MXM with 5 nm interlayers (R ~ 0.369). Despite

the fact that thicker barriers can increase the stability of the Sc/Si mirrors, it can be seen from the figure that this will be mainly at the expense of reflectivity.

In Fig. 7b similar calculations are presented, but with barriers only at single-type interfaces. It can be visible here that the use of carbon barriers at the Sc-on-Si (C-on-Si) interfaces leads to a larger drop in the peak reflectivity with the carbon layer thickness (R: 0.378 $\to$ 0.334). At the same time, the MXM with thin barrier layers still has an advantage over the Sc/Si MXM with 5 nm silicide interlayers. However, even the insertion of thin barriers onto the Si-on-Sc (C-on-Sc) interfaces leads to an increase in the peak reflectivity up to $R \sim 0.432$ ($t_C \sim$ 0.2 nm) compared to the reference mirror with 3 nm interlayers. At $t_C \sim 0.65$ nm the reflectivity grows a little bit more (up to $R \sim 0.437$). We would like to notice that the total increase in the reflectivity for mirrors with barriers at the Si-on-Sc interface is ~ 1.6 %, in spite of the fact that the total thickness of the barrier layer becomes comparable with the thickness of the silicide layer.

Thus, the barrier layers of carbon decrease the interlayer thickness and can be used to enhance the reflectivity of the Sc/C/Si multilayer mirrors with moderate effect.

4. Conclusions

The use of carbon as barrier layers for Sc/Si multilayer X-ray mirrors has been studied. Carbon reacts with scandium and silicon layers at the deposition stage forming carbides. Thin ScC layers ($t_{ScC} <$ 1.9 nm at Si-on-Sc interfaces) isolate the Sc and Si layers partially. When $t_C > 0.65$ nm thicker ScC layers separate the matrix layers completely, however the excess carbon interacts with the deposited silicon layers forming the silicon carbide layer. Thin SiC layers (Sc-on-Si interfaces) up to ~ 0.9 nm are unstable, and the scandium deposited thereupon decomposes it and reacts with both silicon and carbon, transforming SiC layers into carbide-silicide layers (ScC and ScSi) with up to ~ 2.6 nm thickness ($t_{ScC} \sim$ 0.4 nm). Thinner carbide-silicide layer is also semitransparent. At thicknesses $t_{ScC} >$ 0.4 nm, carbon separates the Sc and Si layers completely (Sc-on-Si interfaces) and can be in the free state but reacts with the scandium deposited on it.

Due to the use of carbon barrier layers, the width of the interlayers can be reduced at least by ~ 15 %. Estimates show that it is possible to increase the reflectivity of the Sc/C/Si MXMs at the wavelength of $\lambda \sim$ 46 nm if the carbon is deposited only at the Si-on-Sc interface.

Critical thicknesses of carbon layers at which they completely isolate the Sc and Si layers are established. Further studies are in progress to determine the efficient temperature range for utilization of the Sc/Si MXMs with carbon barrier layers.

Acknowledgments. YPP is acknowledged ISKCON for understanding the place and value of this work.

References

1. Yu.A.Uspenskii, V.E.Levashov, A.V.Vinogradov et al., *Opt.Lett.*, **23**, 771 (1998).
2. S.Bajt, J.B.Alameda, W.M.Clift et al., *Opt. Eng.*, **41**, 1797 (2002).
3. S.Braun, H.Mai, M.Moss et al., *Jpn.J.Appl. Phys.*, **41**, 4074 (2002).
4. S.Yulin, F.Schafers, T.Feigl et al., *Proc. SPIE*, **5193**, 155 (2004).
5. J.Gautier, F.Delmotte, M.Roulliay et al., *Proc. SPIE*, **5963**, 56930X (2005).
6. C.D,Macchietto, B.R.Benware, J.J.Rocca, *Opt. Lett.*, **24**, 1115 (1999)
7. A.V.Vinogradov, J.J.Rocca, *Quant. Electron.*, **33**, 7 (2003).
8. H.Takenaka, T.Kawamura, *J.Electron.Spectrosc.Relat.Phenom.*, **80**, 381 (1996).
9. M.Moss, T.Bottger, S.Braun et al., *Thin Solid Films*, **468**, 322 (2004).
10. A.V.Penkov, E.N.Zubarev, O.V.Poltseva et al., *PAST*, No. 4, 157 (2006).
11. A.Kubec, J.Maser, P.Formanek et al., *Appl. Phys.Lett.* **110**, 111905 (2017).
12. D.L.Windt, *Comput.Phys.*, No. 4, 360 (1998).
13. Yu.A.Uspenskii, J.F.Seely, N.L.Popov et al., *J.Opt.Soc.Am.A*, **21**, 298 (2004).
14. M.Fernandez-Perea, J.I.Larruquert, J.A.Aznarez et al., *J.Opt.Soc.Am.A*, **23**, 2880 (2006).
15. Y.P.Pershyn, E.N.Zubarev, D.L.Voronov et al., *J.Phys.D:Appl.Phys.*, **42**, 125407 (2009).
16. D.L.Windt, S.Donguy, J.Seely et al., *Appl. Opt.*, **43**, 1835 (2004).
17. Specular X-ray Optics, ed. by A.V.Vinogradov, Mashinostroenie, Leningrad (1989) [in Russian].
18. R.Pottgen, W.Jeitschko, *Inorg.Chem.*, **30**, 427 (1991).